PHYSICS AND CHEMISTRY OF SOLIDSTATE
V. 18, № 2 (2017) P. 222-227
DOI: 10.15330/pcss.18.2.222-227

ФІЗИКА І ХІМІЯ ТВЕРДОГО ТІЛА
Т. 18, № 2 (2017) С. 222-227

UDK 680.18:669.71

ISSN 1729-4428

O.V. Sukhova, V.A. Polonskyy, K.V. Ustinova

Structure Formation and Corrosion Behaviour of Quasicrystalline Al–Ni–Fe Alloys

The Oles' Honchar Dnipropetrovs'k National University, 72 Gagarin Ave, Dnipro, 49010, aspkat@i.ua

The formation of quasicrystalline decagonal phase and related crystalline phases was investigated by a combination of optical metallography, powder X-ray diffraction, atomic absorption spectroscopy and differential thermal analysis. Corrosion behaviour of quasicrystal Al–Ni–Fe alloys was studied by gravimetric and potentiodynamic polarization experiments in saline and acidic solutions at room temperature. The decagonal phase exhibits two modifications (AlFe- and AlNi-based) depending on the composition. In $Al_{72}Ni_{13}Fe_{15}$ alloy it coexists with monoclinic Al_5FeNi phase. In $Al_{71.6}Ni_{23}Fe_{5.4}$ alloy crystalline $Al_{13}(Ni,Fe)_4$, $Al_3(Ni,Fe)_2$, and $Al_3(Ni,Fe)$ phases are seen adjacent to the quasicrystalline decagonal phase. Stability of quasicrystal phase up to room temperature was shown to be connected with its incomplete decomposition during cooling at a rate of 50 K/min. $Al_{72}Ni_{13}Fe_{15}$ alloy has more than twice larger volume fraction of this phase compared to that of $Al_{71.6}Ni_{23}Fe_{5.4}$ alloy. A dependence of microhardness on composition was observed as well, with $Al_{72}Ni_{13}Fe_{15}$ alloy having substantially higher values. In acidic solutions, $Al_{71.6}Ni_{23}Fe_{5.4}$ alloy showed the best corrosion performance. In saline solutions, the investigated alloys remained mainly untouched by corrosion. Mass-change kinetics exhibited parabolic growth rate. After a potentiodynamic scan in 3.0 M NaCl solution polarization of $Al_{72}Fe_{15}Ni_{13}$ and $Al_{71.6}Ni_{23}Fe_{5.4}$ alloys revealed that stationary potential values became more negative, with anodic process slowed down. The polarization curves showed that both the quasicrystalline alloys turned to passive state in this solution.

Key words: decagonal phase, microstructure, corrosion behaviour, stationary potential, electrochemical passivity zone.

Article acted received 13.02.2017; accepted for publication 05.06.2017.

Introduction

Al–Fe–Ni alloys have been applied as the basis of the Alnico magnets due to their magnetic properties [1], and as high-temperature materials thank to high melting temperature [2, 3]. Besides, Al–Fe–Ni alloys show very attractive properties for applications in industrial furnaces [4] and petroleum chemical plants [5] by alloying with Cr (up to 8 at. %) or Hf (up to 0.1 at. %). Al–Fe–Ni alloys produced by mechanical alloying can be employed as catalyzers, with aluminum leached by neutralizing water solution [6]. The alloys of the said system in the concentration range of quasicrystalline decagonal D-phase formation are of a special interest. This phase is a two-dimensional quasicrystal consisting of periodic stacking of atomic layers with a tenfold symmetry within the plane. Decagonal quasicrystals combine two types of crystalline order: they are quasiperiodic in a plane and they are periodic in the direction perpendicular to a plane.

The D-phase stability at room temperature is still under discussion. A quasicrystalline decagonal phase was found to form at compositions very close to $Al_{72}Ni_{13}Fe_{15}$ and $Al_{71.6}Ni_{23}Fe_{5.4}$ [7, 8]. In a review paper [9] it was asserted that decagonal quasicrystals in the Al–Ni–Fe system are to be regarded as metastable. It was suggested that the decagonal phase appears as an intermediate state during the formation of $Al_{13}(Fe,Ni)_4$ from the liquid. According to several studies it is stable within a narrow compositional range of $Al_{71.1\text{-}71.7}Ni_{24.6\text{-}23.0}Fe_{4.3\text{-}5.3}$ [10–12]. In other works [13–15] D-phase is assumed to be thermodynamically stable between 930 and 847 °C, and on further cooling transforms to the mixture of three crystalline phases. Besides, in the study [8] the formation of a single decagonal D-phase by rapid solidification is reported to occur in the concentration range of $Al_{75\text{-}70}Ni_{16\text{-}9}Fe_{9\text{-}21}$. In papers [16–19] the formation of stable D-phase is confirmed as well.

For any applications of quasicrystals, corrosion resistance is of utmost importance. Therefore, the aim of this paper is to investigate structure and corrosion properties of as-cast Al–Ni–Fe alloys for chemical

compositions set closely to the compositions, where the quasicrystal decagonal D-phase has been observed.

I. Experimental procedure

The alloys with nominal compositions of $Al_{72}Fe_{15}Ni_{13}$ and $Al_{71.6}Ni_{23}Fe_{5.4}$ were prepared of high purity (99.99 pct.) aluminum, nickel, and iron. These elements were put in a graphite crucible and melted using Tamman furnace. The cooling rate of the alloys was 50 K/min. The average chemical composition of the alloys was studied by atomic absorption spectroscopy method using *Sprut СЕФ-01-М* device. The alloys were examined by light-optical microscope *Neophot*. Quantitative metallography was carried out with structural analyzer *Epiquant*. X-ray diffraction analysis was done to identify the existing phases in produced samples on an X-ray diffractometer *ДРОН-УМ-1* with CuK_α source. The reactions involving the decagonal quasicrystalline phase were investigated by means of differential thermal analysis (DTA). DTA measurements were carried out using open alumina crucibles. Two heating and cooling curves were recorded for each sample at a heating rate of 5 K/min. Vickers microhardness was measured by using a diamond indenter under a 50 gf load. Corrosion behaviour was investigated by gravimetric method in chloric, sulphate, nitrate or orthophosphoric acidic solutions (pH = 1.0) for 1 to 4 hours and sodium chloride or sodium sulphate saline solutions (pH = 7.0) for 1 to 4 days. The polarization experiments were conducted by means of *ПІ–50–1* potentiostat and *ПР–8* programmer using three-electrode electrolytic cell. Platinum was selected as reference electrode, silver chloride – as working electrode. While volt-ampere diagrams were registered, a potential was scanned from its stationary value to the cathodic or anodic region at the rate of 1.0 mV/s. Corrosion and electrochemical tests were carried out at the temperature of 20 ± 2ºC.

II. Experimental results and discussion

$Al_{72}Fe_{15}Ni_{13}$ alloy exhibits two-phase structure (Fig. 1). From X-ray diffraction patterns the investigated samples consist of primary Al_5FeNi phase separated by

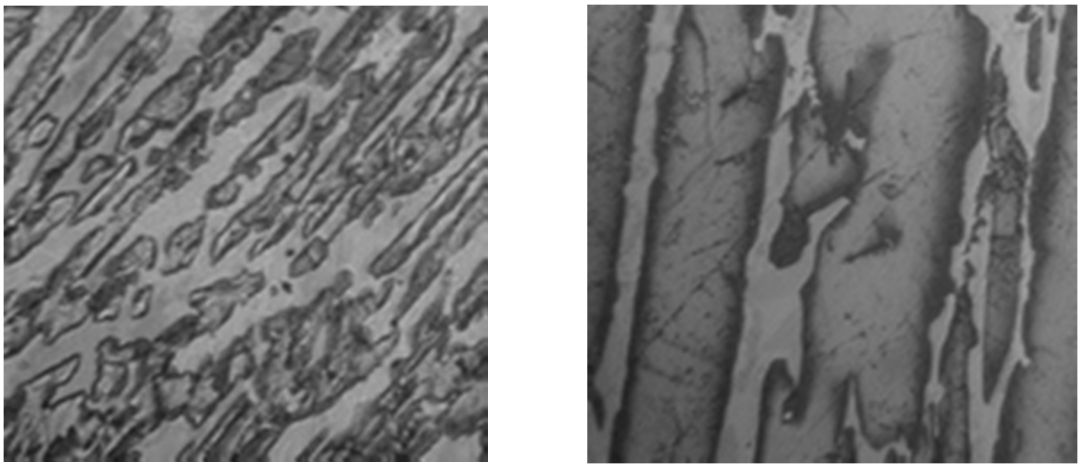

a **b**

Fig. 1. Microstructure of $Al_{72}Fe_{15}Ni_{13}$ alloy: a – x 200; b – x 400.

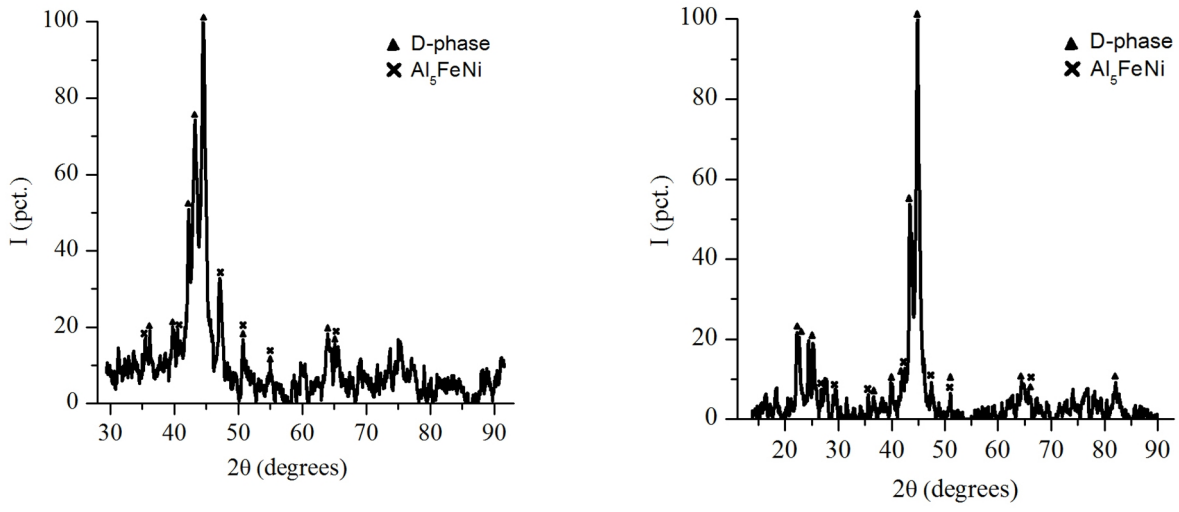

a **b**

Fig. 2. Diffraction patterns of $Al_{72}Fe_{15}Ni_{13}$ alloy: a – before DTA; b – after DTA.

secondary quasicrystalline decagonal D-phase as shown in Fig. 2. Thermal effects represented by DTA results indicate the formation of D-phase at 930 °C and Al_5FeNi at 1070 °C (Fig. 3, a).

The volume fraction of D-phase reaches 32.0 vol. pct. of a total alloy volume (Table 1). D-phase of $Al_{72}Fe_{15}Ni_{13}$ alloy corresponds to a solid solution of nickel in $Al_{86}Fe_{14}$ (D-AlFe type) [7].

$Al_{71.6}Ni_{23}Fe_{5.4}$ alloy consists of three phases identified as quasicrystalline decagonal D-phase,

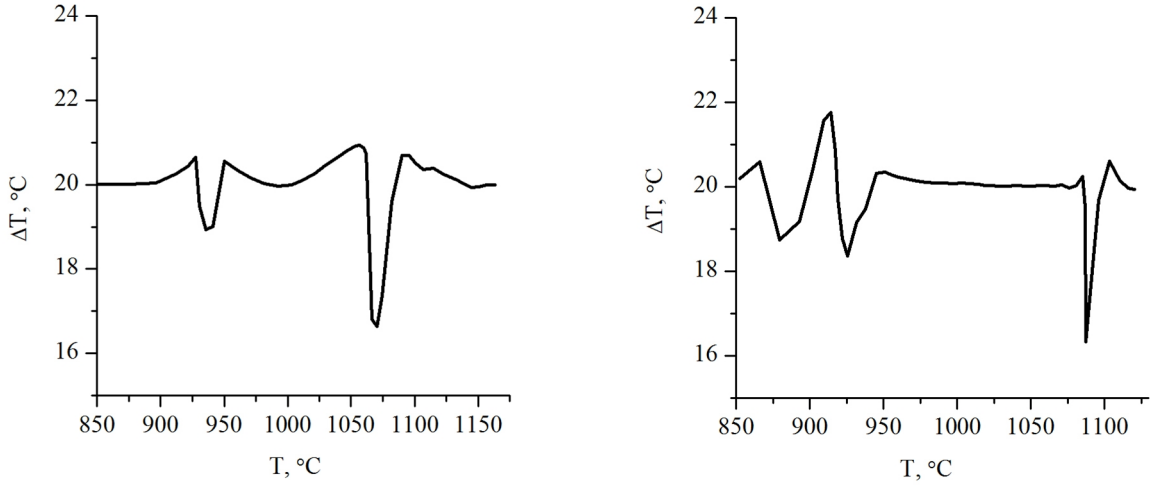

a **b**

Fig. 3. DTA cooling curves of the following alloys: a –$Al_{72}Fe_{15}Ni_{13}$; b – $Al_{71.6}Ni_{23}Fe_{5.4}$.

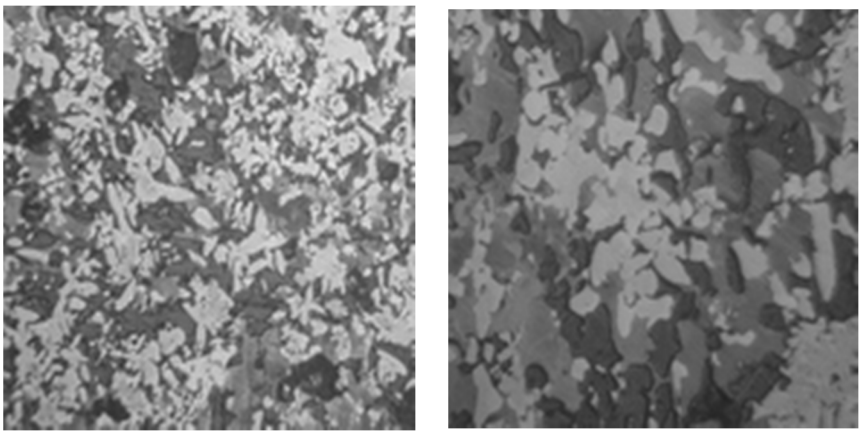

a **b**

Fig. 4. Microstructure of $Al_{71.6}Ni_{23}Fe_{5.4}$ alloy: a – x 200; b – x 400.

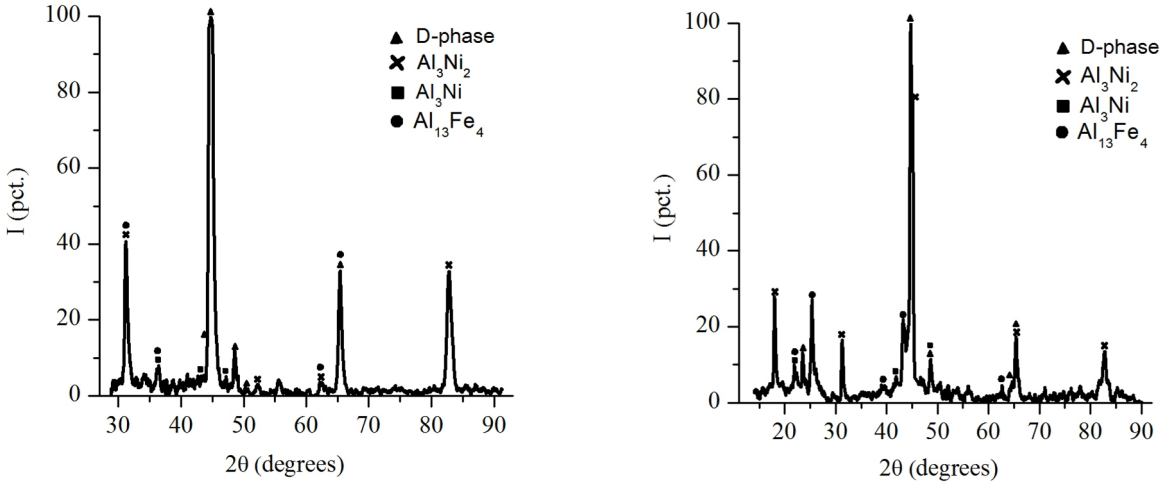

a **b**

Fig. 5. Diffraction patterns of $Al_{71.6}Ni_{23}Fe_{5.4}$ alloy: a – before DTA; b – after DTA.

monoclinic $Al_{13}(Ni, Fe)_4$ phase, hexagonal $Al_3(Ni, Fe)_2$ phase, orthorombic $Al_3(Ni, Fe)$ phase (Fig. 4). After etching dark-colored quisicrystalline D-phase takes about 13.7 pct. of a total alloy volume (Table 1).The described phase composition is confirmed by X-ray investigations (Fig. 5). At 925–930 °C the decagonal phase was in equilibrium with the liquid and $Al_3(Ni,Fe)_2$, and at 875 – 885 °C with $Al_{13}(Ni,Fe)_4$, $Al_3(Ni,Fe)_2$, and $Al_3(Ni,Fe)$ due to its decomposition to the mentioned three crystalline phases upon cooling. A summary of the reactions temperatures derived from DTA data is given in Fig. 3, b. D-phase of $Al_{71.6}Ni_{23}Fe_{5.4}$ alloy corresponds to a solid solution of iron in $Al_{80}Ni_{20}$ (D-AlNi type) [7].

Thus, analysis of the as-cast $Al_{72}Fe_{15}Ni_{13}$ and $Al_{71.6}Ni_{23}Fe_{5.4}$ alloys revealed that some quantity of the decagonal phase formed during solidification can remain down to room temperature. These results point to the possibility of extending the temperatural limits of the decagonal phase by cooling at 50 K/min. The volume fraction of D-phase of $Al_{71.6}Ni_{23}Fe_{5.4}$ alloy is more than 2 times higher than that of $Al_{72}Fe_{15}Ni_{13}$ alloy. The total microhardness of $Al_{72}Fe_{15}Ni_{13}$ alloy exceeds that of $Al_{71.6}Ni_{23}Fe_{5.4}$ alloy (Table 1). Besides, measurements showed that the decagonal D-quasicrystals of $Al_{72}Fe_{15}Ni_{13}$ alloy possess a higher microhardness than those of $Al_{71.6}Ni_{23}Fe_{5.4}$ alloy.

Table 1

Summary of the quantitative metallographic analysis and microhardness measurements of the as-cast Al–Ni–Fe alloys

Alloy	D-phase volume fraction, pct.	D-phase microhardness, GPa	Total microhardness of alloy, GPa
$Al_{72}Fe_{15}Ni_{13}$	32.0 ± 0.1	10.8 ± 1.33	10.1 ± 0.7
$Al_{71.6}Ni_{23}Fe_{5.4}$	13.7 ± 0.1	9.2 ± 0.47	4.9 ± 0.3

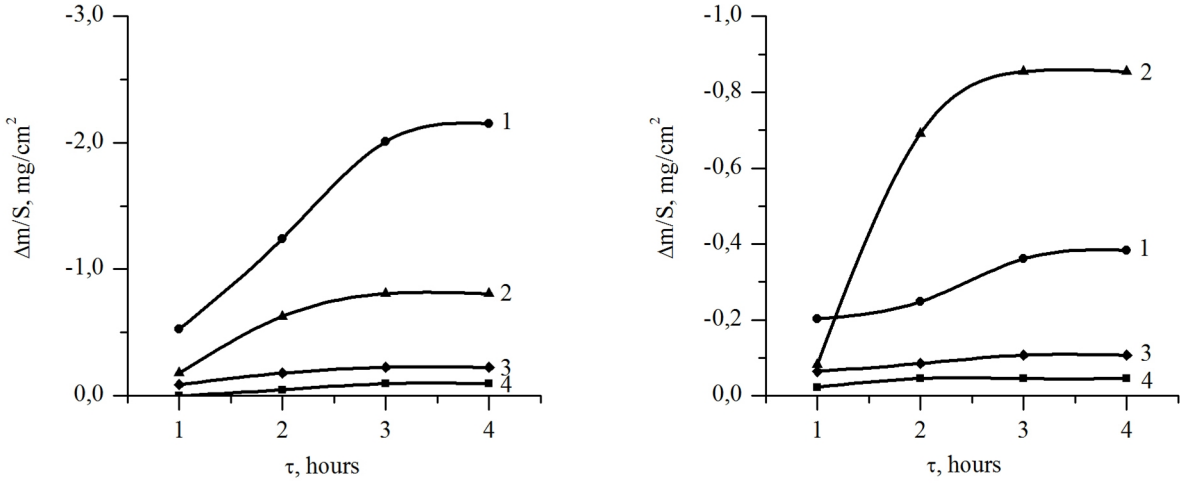

Fig. 6. Mass change per unit area vs. corrosion time for $Al_{72}Fe_{15}Ni_{13}$ (a) and $Al_{71.6}Ni_{23}Fe_{5.4}$ (b) alloys in acidic solutions (pH=1.0): 1 – H_3PO_4; 2 – H_2SO_4; 3 – HCl; 4 – HNO_3.

Table 2

Relative mass change for $Al_{72}Fe_{15}Ni_{13}$ and $Al_{71.6}Ni_{23}Fe_{5.4}$ alloys vs. corrosion time in saline solutions, %

Alloy	Solution	Corrosion time, days			
		1	2	3	4
$Al_{72}Fe_{15}Ni_{13}$	0.4 M Na_2SO_4	0.1	0.2	0.2	0.2
	3.0 M NaCl	0.0	0.0	0.0	0.1
$Al_{71.6}Ni_{23}Fe_{5.4}$	0.4 M Na_2SO_4	0.0	0.1	0.1	0.1
	3.0 M NaCl	0.0	0.0	0.0	0.0

The composition and microstructure of the investigated alloys are the key parameters defining their corrosion and electrochemical behaviour. Fig. 6 shows the results of the corrosion tests plotting mass change per unit area vs. corrosion time in acidic solutions (pH = 1.0). The best corrosion performance in acidic solutions exhibits $Al_{71.6}Ni_{23}Fe_{5.4}$ alloy for which maximum mass loss in sulphate acid solution reaches 0.8 mg/cm^2 for 4 hours. The poorer resistance to corrosion shows $Al_{72}Fe_{15}Ni_{13}$ alloy for which maximum mass loss reaches 2.1 mg/cm^2 in orthophosphoric acidic solutions. Both the alloys do not practically react with chloric and nitrate acidic solutions.

The investigated alloys do not noticeably corrode in Na_2SO_4 and NaCl saline solutions (Table 2). Their colour and mass do not essentially change. This may be

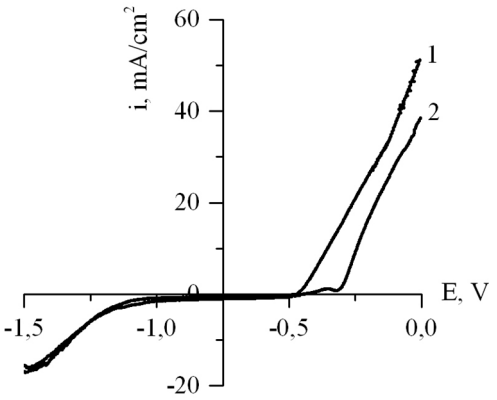

Fig. 7. Polarization curves in 3.0 M NaCl solution (pH=7.0) for the following alloys: 1 – $Al_{72}Fe_{15}Ni_{13}$; 2 – $Al_{71.6}Ni_{23}Fe_{5.4}$.

explained by transition of the alloys to passive state due to nickel present in their composition.

The inertness of the investigated alloys in neutral media may be substantiated by measuring stationary potential (E) values by means of long-term registration of (E, τ)–dependencies in 3.0 M NaCl solution (pH = 7.0). The increase in nickel content from 13 to 23 at. % is established to shift stationary potential to more positive values from –0.55 V to -0.46 V. These results indicate that $Al_{71.6}Ni_{23}Fe_{5.4}$ alloy is more electrochemically inert than $Al_{72}Fe_{15}Ni_{13}$ alloy.

The further polarization measurements were conducted to determine electrochemical passivity zones of the alloys beyond which water reduction with hydrogen liberation takes place in the cathodic region or alloy oxidation and oxygen emission proceed in the anodic region. The polarization rate during the measurements was 1 mV/s, i.e. (i, E)–dependencies for both alloys were registered practically in stationary conditions. As shown in Fig. 7, cathode current density (i) for the alloys is equally started to increase at potentials more negative than -1.0 V. In the anodic region of polarization curves, passivity zones disappear at 0.47 V for $Al_{72}Fe_{15}Ni_{13}$ alloy and at 0.32 V for $Al_{71.6}Ni_{23}Fe_{5.4}$ alloy. Thus, the increase in a nickel content of the alloys promotes slowdown of anodic process, with alloys becoming more inert.

Conclusions

1. Quasicrystalline decagonal D-phase was observed in the structure of Al–Ni–Fe alloys with the compositions of $Al_{72}Fe_{15}Ni_{13}$ and $Al_{71.6}Ni_{23}Fe_{5.4}$ cooled at a rate of 50 K/min. The decagonal phase was established to exhibit two modifications (AlFe- and AlNi-based) depending on the alloy composition. This phase of $Al_{72}Fe_{15}Ni_{13}$ alloy is based on binary quasicrystalline $Al_{86}Fe_{14}$ compound and at room temperature coexists with crystalline hexagonal Al_5FeNi phase, and D-phase of $Al_{71.6}Ni_{23}Fe_{5.4}$ alloy is based on $Al_{80}Ni_{20}$ and coexists with three crystalline phases as follows: monoclinic $Al_{13}(Ni, Fe)_4$, hexagonal Al_3Ni_2, orphorombic $Al_3(Ni, Fe)$ phases.

2. Al–Ni–Fe alloys do not essentially corrode in neutral saline solutions and chloric or nitrate highly acidic solutions. In sulphate and orthophosphoric acidic solutions corrosion activity of the alloys is low and decreases with increasing nickel content of the alloy due to surface passivation. For $Al_{72}Fe_{15}Ni_{13}$ alloy as compared to $Al_{71.6}Ni_{23}Fe_{5.4}$ alloy, stationary potential values become more negative and electrochemical passivity zone extends due to anodic processes slowdown.

Sukhova O.V. - Professor, Doctor of Technical Sciences, Department of Experimental Physics and Metal Physics;
Polonskyy V.A. – Ph.D (chemical sciences), associate professor, associate professor of the department of physical and inorganic chemistry;
Ustinova K.V. - Engineer of the Department of Experimental Physics and Metal Physics.

.

[1] G. Marcon, S. Lay, Ann. Chim. Sci. Mater. 25(1), 21 (2000).
[2] H. Bitterlich, W. Loeser, L. Schultz, J. Phase Equilib. 23(4), 301 (2002).
[3] R. Rablbauer, G. Frommeyer, F. Stein, Mater. Sci. Eng. A 343(1–2), 301 (2003).
[4] G. Sauthoff, Intermetallics (Verlag Chemie, Weinheim, 1995).
[5] G. Sauthoff, Intermetallics 8(9–11), 1101 (2000).
[6] B.H. Zeifert, J. Salmones, J.A. Hernandez, R. Reynoso, N. Nava, E. Reguera, J.G. Cabanas-Moreno, G. Aguilar-Rios, J. Radioanal. Nucl. Chem. 245(3), 637 (2000).
[7] J.-B. Qiang, D.-H. Wang, C.-M. Bao, Y.-M. Wang, W.-P. Xu, M.-L. Song, C. Dong, J. Mater. Res. 16(9), 2653 (2001).
[8] A.D. Setyawan, D.V. Louzguine, K. Sasamori, H.M. Kimura, S. Ranganathan, A. Inoue, J. Alloys and Compounds 399(1–2), 132 (2005).
[9] G. T. de Laissardiere, D. Nguyen-Manh, D. Mayou, Progress in Materials Science 50(6), 679 (2005).
[10] B. Grushko, K. Urban, J. Phil. Mag. B. 70(5), 1063 (1994).
[11] B. Grushko, T. Velikanova, Computer Coupling of Phase Diagrams and Thermochemistry 31, 217 (2007).
[12] I. Chumak, K. W. Richter, H. Ipser, Intermetallics. 15(11), 1416 (2007).
[13] L. Zhang, Y. Du, H. Xu, C. Tang, H. Chen, W. Zhang, J. Alloys and Compounds 454(1–2), 129 (2008).
[14] U. Lemmerz, B. Grushko, C. Freiburg, M. Jansen, Phil. Mag. Let. 69(3), 141 (1994).

[15] B. Grushko, U. Lemmerz, K. Fischer, C. Freiburg, Phys. Stat. Sol. 155(17), 17 (1996).
[16] O.V. Sukhova, Yu.V. Syrovatko, K.V. Ustinova, Visnik Dnipropetrovs'kogo universitetu. Seria Fizika, radioelektronika 22(1), 112 (2014).
[17] Е.В. Суховая, В.Л. Плюта, Е.В. Устинова, Фундаментальные и прикладные проблемы черной металлургии 29, 202 (2014).
[18] V.F. Bashev, O.V. Sukhova, K.V. Ustinova, Строительство, материаловедение, машиностроение 74, 3 (2014).
[19] O.V. Sukhova, K.V. Ustinova, Visnik Dnipropetrovs'kogo universitetu. Seria Fizika, radioelektronika 23(1), 60 (2015).

О.В. Сухова, В.А. Полонський, К.В. Устінова

Структуроутворення та корозійні властивості квазікристалічних сплавів Al–Ni–Fe

Дніпропетровський національний університет імені Олеся Гончара, пр. Гагаріна, 72, м. Дніпро, Україна, 49010, aspkat@i.ua

Досліджено процеси структуроутворення квазікристалічної та співіснуючих кристалічних фаз із застосуванням методів оптичної металографії, рентгеноструктурного, рентгенофлюресцентного і диференціального термічного аналізів. Корозійні властивості сплавів досліджували гравіметричним та потенціодинамічним методами в розчинах солей та кислот за кімнатної температури. Встановлено формування двох модифікацій декагональної квазікристалічної фази (AlFe- і AlNi-тип) залежно від складу. В сплаві $Al_{72}Ni_{13}Fe_{15}$ вона співіснує з моноклінною фазою Al_5FeNi, а у сплаві $Al_{71,6}Ni_{23}Fe_{5,4}$ – з кристалічними фазами $Al_{13}(Ni,Fe)_4$, $Al_3(Ni,Fe)_2$ і $Al_3(Ni,Fe)$. Показано, що стабільність квазікристалічної декагональної фази до кімнатної температури може бути пов'язана з її неповним розпадом при охолодженні зі швидкістю 50 К/хв. Об'ємний вміст декагональної фази у сплаві $Al_{72}Ni_{13}Fe_{15}$ більш ніж у два рази перевищує вміст цієї фази у сплаві $Al_{71,6}Ni_{23}Fe_{5,4}$. Від складу сплаву також залежить мікротвердість, причому загальна мікротвердість сплаву $Al_{72}Ni_{13}Fe_{15}$ суттєво вища. У розчинах кислот найвищу корозійну стійкість має сплав $Al_{71,6}Ni_{23}Fe_{5,4}$. У розчинах солей досліджені сплави майже не кородують. Залежність питомої зміни маси зразків від часу корозії має параболічний характер. При переході від сплаву $Al_{72}Fe_{15}Ni_{13}$ до сплаву $Al_{71,6}Ni_{23}Fe_{5,4}$ стаціонарний електрохімічний потенціал у розчині 3,0 М NaCl має менш від'ємні значення, а зона електрохімічної пасивності розширюється за рахунок гальмування анодних процесів. Обидва досліджені сплави переходять у пасивний стан у цьому розчині.

Ключові слова: декагональна фаза, мікроструктура, корозійна поведінка, стаціонарний потенціал, зона електрохімічної пасивності.